Measurements and Quasi-Quantum Modeling of the Steric Asymmetry and Parity Propensities in State-to-State Rotationally Inelastic Scattering of NO ($^2\Pi_{1/2}$) with D_2†

Craig A. Taatjes

Combustion Research Facility, Mail Stop 9055, Sandia National Laboratories, Livermore, California 94551

Arjan Gijsbertsen

FOM Instituut voor Atoom en Molecuul Fysica (AMOLF), Kruislaan 407, 1098 SJ Amsterdam, The Netherlands

Marc J. L. de Lange‡ and Steven Stolte*

Laser Centre and Department of Physical Chemistry, Faculty of Exact Sciences, Vrije Universiteit, De Boelelaan 1083, 1081 HV Amsterdam, The Netherlands

Received: February 13, 2007; In Final Form: April 4, 2007

Relative integrated cross sections are measured for spin−orbit-conserving, rotationally inelastic scattering of NO ($^2\Pi_{1/2}$), hexapole-selected in the upper Λ-doublet level of the ground rotational state ($j = 0.5$), in collisions with D_2 at a nominal energy of 551 cm^{-1}. The final state of the NO molecule is detected by laser-induced fluorescence (LIF). The state-selected NO molecule is oriented with either the N end or the O end toward the incoming D_2 molecule by application of a static electric field **E** in the scattering region. This field is directed parallel or antiparallel to the relative velocity vector **v**. Comparison of signals taken for the different applied field directions gives the experimental steric asymmetry SA, defined by $SA = (\sigma_{\mathbf{v}\uparrow\downarrow\mathbf{E}} - \sigma_{\mathbf{v}\uparrow\uparrow\mathbf{E}})/(\sigma_{\mathbf{v}\uparrow\downarrow\mathbf{E}} + \sigma_{\mathbf{v}\uparrow\uparrow\mathbf{E}})$, which is equal to within a factor of −1 to the molecular steric effect, $S_{i\rightarrow f} \equiv (\sigma_{D_2\rightarrow NO} - \sigma_{D_2\rightarrow ON})/(\sigma_{D_2\rightarrow NO} + \sigma_{D_2\rightarrow ON})$. The dependence of the integral inelastic cross section on the incoming Λ-doublet component is also measured as a function of the final rotational (j_{final}) and Λ-doublet (ϵ_{final}) state. The measured steric asymmetries are similar to those previously observed for NO−He scattering. Spin−orbit manifold-conserving collisions exhibit a larger propensity for parity conservation than their NO−He counterparts. The results are interpreted in the context of the recently developed quasi-quantum treatment (QQT) of rotationally inelastic scattering [Gijsbertsen, A.; Linnartz, H.; Taatjes, C. A.; Stolte, S. *J. Am. Chem. Soc.* **2006**, *128*, 8777]. The QQT predictions can be inverted to obtain a fitted hard-shell potential that reproduces the experimental steric asymmetry; this fitted potential gives an empirical estimate of the anisotropy of the repulsive interaction between NO and D_2. QQT computation of the differential cross section using this simple model potential shows reasonable agreement with the measured differential cross sections.

Introduction

Owing to the feasibility of completely state-resolved experiments, inelastic scattering can be a detailed probe of interaction potentials[1] and can test theoretical descriptions of molecular collisions. Collisions of open-shell molecules such as nitric oxide, NO, are especially important in testing theoretical methods. The spectroscopy of NO is well-developed, and state-specific detection of scattered products is readily achievable. Additionally, it is possible to select a single rotational and Λ-doublet state of NO from a molecular beam with a hexapole state selector and to subsequently orient the axis of the state-selected NO molecule in the laboratory frame by application of a static electric field.[2−4] Scattering from such a prepared state permits the measurement of the steric asymmetry in inelastic scattering,[3−8] that is, the difference in scattering efficiency between collisions on the two ends of the molecule, depending on whether the applied electric field is parallel or antiparallel to the relative velocity.

The steric asymmetry in the rotationally inelastic scattering of NO with He[9] and with Ar[5,6,10] has previously been measured and compared with detailed quantum chemical calculations. A marked oscillation in the orientation dependence of the inelastic scattering is observed as a function of final rotational state, with even Δj ($= j_{final} - j_{initial}$) transitions greatly enhanced by application of an electric field antiparallel to the relative velocity (N end collisions) and odd Δj transitions preferring an electric field parallel to the relative velocity (O end collisions). Aside from a tenacious and irksome discrepancy in the sign of the steric asymmetry,[9,11−13] the orientation dependence is reliably reproduced by detailed calculations. The identification of N and O end scattering above assumes an electric dipole ($N^{\delta-}O^{\delta+}$)[14] and produces disagreement with theory by a factor of −1 for the steric asymmetry. Test calculations have shown that the alternation of steric effect arises primarily from short-range anisotropic terms,[10] and the observed asymmetry in the scattering

† Part of the "Roger E. Miller Memorial Issue".

* To whom correspondence should be addressed. E-mail: stolte@few.vu.nl.

‡ Present address: Swammerdam Institute for Life Sciences, University of Amsterdam, P.O. Box 94062, 1090 GB Amsterdam, The Netherlands.

10.1021/jp0712405 CCC: $37.00
Published on Web 06/02/2007

of NO with He, where repulsive interactions dominate, is substantially larger than that for NO scattering from Ar.[6,9]

The interaction potential of He−NO and D_2−NO was investigated by Butz et al.,[15] who measured the velocity dependence of the total scattering cross section. They noted a well-developed $N = 1$ glory maximum in D_2−NO near a relative velocity of 1500 m s^{-1} but only a weak indication of a glory maximum in He−NO, at much lower velocity. The first measurements of the rotationally inelastic differential cross sections for D_2−NO collisions were carried out by Westley et al.[16] In their experiments, an expansion-cooled beam of NO ($j = 1/2, 3/2$; $\Pi_{1/2}$) molecules was crossed by an expansion-cooled beam of D_2 molecules. The scattered NO molecules, in individual final spin-orbit, rotational, and Λ-doublet levels, were ionized by 1 + 1 resonance-enhanced multiphoton ionization (REMPI) via the $\gamma(0,0)$ band near 226 nm, and their velocity distribution was detected by velocity-map ion imaging. Fully final-state-selected differential cross sections were extracted from the resulting ion images. Scattering from D_2 was slightly more forward than that from He for a given final j state. These differences were attributed partially to differences in the interaction potential between the two systems and partially to a small difference in collision energy. Gijsbertsen et al. recently measured final-state-resolved differential cross sections for scattering of fully initial-state-selected NO ($|j\ m_j\ \bar{\Omega}\ \epsilon\rangle = |1/2\ \pm 1/2\ 1/2\ -1\rangle$) with He[17] and with D_2.[18] The notation $\bar{\Omega}$ indicates the absolute value of Ω. In their experiments, carried out at similar collision energies to the Westley et al. measurements (and to the present work), they also observed a shift toward forward scattering in moving from He to D_2. They suggested[18] that the differences in the rainbow angles could reflect a larger anisotropy in the D_2−NO interaction than that for He−NO but shrank somewhat from this conclusion because of the similar maximum j_{final} observed in the two systems.

The present work investigates steric effects in inelastic scattering of NO and D_2 and interprets the results using a hard-shell model and the recently developed "Quasi-quantum treatment" (QQT) of rotationally inelastic scattering.[12] The steric asymmetry is reported for spin−orbit-conserving inelastic collisions of NO with D_2. The predictions of QQT are used to fit a model hard-shell potential for D_2−NO that reproduces the observed steric effects. The differential cross sections for NO ($|j\ m_j\ \bar{\Omega}\ \epsilon\rangle = |1/2\ \pm 1/2\ 1/2\ -1\rangle$)−$D_2$ scattering[18] are also compared with predictions from QQT, using the model hard-shell potential.

Methods

Experiment. The measurement of steric effects in D_2−NO scattering was carried out in the same manner as that from previously reported investigations of He−NO collisions.[9] Because the collisional kinematics of the two systems are nearly identical, the same experimental configuration was used for the present experiments as that for the He−NO scattering. The pulsed crossed-molecular-beam scattering apparatus is similar to that described in earlier studies.[5,6,19] A 16% mixture of NO in Ar was expanded from a stagnation pressure of 3.5 bar through a 0.8 mm diameter orifice in a pulsed (10 Hz) nozzle. The resulting beam was skimmed and passed through a 167 cm long hexapole assembly that focuses NO molecules in the selected $|j\ m_j\ \bar{\Omega}\ \epsilon\rangle = |1/2\ \pm 1/2\ 1/2\ -1\rangle$ state into the scattering center, 293 cm from the pulsed nozzle source.[6] The NO beam was crossed at 90° by a beam of D_2 and expanded through a pulsed nozzle at 5 Hz. The distance from the D_2 pulsed nozzle to the scattering center is 8.4 cm. The speeds of both beams, $\bar{v}_{NO} = 594$ m s^{-1} [9] and $\bar{v}_{D_2} = 1830$ m s^{-1},[16] yielded a nominal center-of-mass collision energy of ∼551 cm^{-1}. The state-selected NO molecules were oriented by a 10 kV cm^{-1} DC electric field that was applied parallel or antiparallel to the relative velocity vector.[6] This applied field created a superposition of parity states with a definite laboratory frame orientation. The coefficients describing this superposition have been experimentally deduced from measurements of LIF intensities of field-induced transitions.[4] Because the NO was in a weak-field seeking state, the negatively charged end of the NO molecule pointed preferentially toward the negative electrodes.

The scattered NO molecules were state-selectively detected by laser-induced fluorescence (LIF) using the frequency-doubled (∼226 nm) output of a Nd:YAG-pumped dye laser operating at 10 Hz. The pulse energy of the laser is typically several hundred microjoules, and the frequency bandwidth is 0.15 cm^{-1} (fwhm). The propagation direction and the linear polarization of the laser lie in the plane of the molecular beams; the laser makes an angle of ∼30° with the relative velocity vector. The fluorescence was collected perpendicular to the plane of the molecular and laser beams, filtered by a cell of liquid CH_2Cl_2, and imaged onto a solar-blind photomultiplier tube (PMT). The PMT voltage was time-gated to reject scattered laser light.

The output of the PMT was collected by a gated integrator and boxcar averager and transferred to a personal computer (PC). As the repetition rate of the secondary beam is half of that of the NO beam and of the laser, the signal with and without the D_2 beam was measured on alternate laser shots. The subtraction of the scattered signal and the baseline signal, yielding the LIF signal for molecules scattered from the prepared initial state to the probed final state $|j_{final}\ \bar{\Omega}_{final}\ \epsilon_{final}\rangle$, was carried out for successive pairs of laser shots in the PC. After 100 pairs of laser pulses in the absence of the orientation field (probing the scattered signal of the pure upper Λ-doublet component), voltage was applied to the orientation electrodes. The scattered signal at one orientation was then collected for 100 pairs of pulses, followed by reversal of the orientation field, a pause of 2 s, and collection of the signal for 100 pairs of pulses at the opposite direction. Finally, the voltage of the orientation field was again set to 0 kV. This cycle was repeated 12−15 times. To eliminate possible bias if the determination of the scattered signal for one orientation was always preceded by the zero-field measurements, the order of the measurements of the two orientations was switched on alternate cycles. For the selected state, with a positive Stark effect, the positively charged end of the molecule was pointed toward the positive electrode. With the electric field defined as pointing from positive to negative polarity (and the relative velocity defined as pointing toward the NO molecule), the LIF signals for the two orientations of the electric field, $I(\mathbf{v}^{\uparrow\uparrow}\mathbf{E}) \equiv I^+$ and $I(\mathbf{v}^{\uparrow\downarrow}\mathbf{E}) \equiv I^-$, are proportional to the relative inelastic cross sections for collisions of D_2 with the positive and negative end of the NO dipole.

The apparatus function relating the LIF intensities to relative inelastic scattering cross sections has been evaluated for the present experimental configuration.[20] The apparatus function slightly favors detection of forward scattered products, but the ratio of LIF signals for the different directions of the applied field should still closely approximate the total steric asymmetry.[9] The angular momentum vector of the scattered product may be aligned,[9,20−23] and this alignment will affect the dependence of the detection probability on the scattering angle.[17] However, the steric asymmetry is obtained from integral cross section measurements that differ only in the incoming orientation of

the NO molecule. Because of partial saturation and because the steric effect changes little over the relevant range of the scattering angle,[10] the effects of the polarized laser detection are expected to be minimal. In the present experiments, the e levels were probed via ($R_{11} + Q_{21}$) lines and the f levels by a combination of R_{21} and ($Q_{11} + P_{21}$) lines. In previous measurements of He−NO scattering,[9] no difference in the apparent SA was measured for redundant Q and (P,R) branch probing, showing that the effect of alignment on the measured steric asymmetry is small.

As in previous work,[9,20] the experimental steric effect, for which the symbol SA is employed, is defined by the difference between the LIF signals for opposite orientations of the static field, normalized by their sum

$$\mathrm{SA} \equiv \frac{\sigma_{\mathbf{v}\downarrow\mathbf{E}} - \sigma_{\mathbf{v}\uparrow\mathbf{E}}}{\sigma_{\mathbf{v}\downarrow\mathbf{E}} + \sigma_{\mathbf{v}\uparrow\mathbf{E}}} \cong \frac{I^- - I^+}{I^- + I^+} \Rightarrow \frac{\sigma_{D_2\rightarrow NO} - \sigma_{D_2\rightarrow ON}}{\sigma_{D_2\rightarrow NO} + \sigma_{D_2\rightarrow ON}} \equiv S_{i\rightarrow f} \quad (1)$$

The statistical spread in the individual measurements of the steric effect (that is, the 12−15 cycles of the orientation of the applied field) is used to derive the experimental precision of the determination of SA. The relationship of the experimental quantity SA to the molecular steric effect $S_{i\rightarrow f}$ requires knowledge of which end of the NO molecule is selected in the collision frame. This, in turn, enables comparison with calculations of the steric effect, which should yield $S_{i\rightarrow f}$ directly. Using the directly measured orientation of the applied static field and the sign of the dipole moment from ab initio calculations, $N^{\delta-}O^{\delta+}$,[14] and assuming no long-range collision-induced reorientation would yield SA ≅ $S_{i\rightarrow f}$ in eq 1. As discussed elsewhere,[9,11,12,20] this assignment results in a disagreement of a factor of −1 between theory and experiment.

As in previous work on He−NO scattering, the measurement of the LIF signal at zero applied field, proportional to the scattering from the selected pure $\epsilon = -1$ state, is combined with the orientation measurements to derive the relative state-to-state inelastic cross sections from individual Λ-doublet levels. The average of the LIF signals at the two directions of the applied field is proportional to the average of the cross sections for scattering from the two initial Λ-doublet states, weighted by the experimentally measured[4] mixing coefficients α and β

$$I^- + I^+ \propto \alpha^2 \sigma_{\epsilon=-1\rightarrow|j_{final}\bar{\Omega}_{final}\epsilon_{final}\rangle} + \beta^2 \sigma_{\epsilon=+1\rightarrow|j_{final}\bar{\Omega}_{final}\epsilon_{final}\rangle} \quad (2)$$

Combining this average with the measured zero-field signal, $I^0 \propto \sigma_{\epsilon=-1\rightarrow|j_{final}\bar{\Omega}_{final}\epsilon_{final}\rangle}$, and assuming that the apparatus function does not change with applied DC field (i.e., the proportionality constants are equal), the ratio of cross sections from the different initial Λ-doublet states to the probed final state can be derived

$$\frac{(I^- + I^+)/2}{I^0} = \frac{\alpha^2 \sigma_{\epsilon=-1\rightarrow|j_{final}\bar{\Omega}_{final}\epsilon_{final}\rangle} + \beta^2 \sigma_{\epsilon=+1\rightarrow|j_{final}\bar{\Omega}_{final}\epsilon_{final}\rangle}}{\sigma_{\epsilon=-1\rightarrow|j_{final}\bar{\Omega}_{final}\epsilon_{final}\rangle}} \quad (3)$$

$$L_{\epsilon_{final}} \equiv \frac{\sigma_{\epsilon=+1\rightarrow|j_{final}\Omega_{final}\epsilon_{final}\rangle}}{\sigma_{\epsilon=-1\rightarrow|j_{final}\Omega_{final}\epsilon_{final}\rangle}} = \frac{\frac{(I^- + I^+)/2}{I^0} - \alpha^2}{\beta^2} \quad (4)$$

The ratio of Λ-doublet cross sections, $L_{\epsilon_{final}}$, is least reliable near $L_{\epsilon_{final}} = 0$. For values of $(I^- + I^+)/I^0$ close to α^2, $L_{\epsilon_{final}}$ is very sensitive to inaccuracies in the computed mixing coefficients and to possible inhomogeneities in the orientation field.[9] The Λ-doublet propensity $L_{\epsilon_{final}}$ as a function of j_{final} is related to the propensity for conservation of the parity p from the initial ($j = 1/2$, $\epsilon = \pm 1$) to the final rotational state of the NO molecule (j_{final}, ϵ_{final}). Parity refers to the behavior of a wave function Ψ upon inversion of all spatial coordinates **r**, $\Psi(-\mathbf{r}) = p\Psi(\mathbf{r})$. The parity of a NO rotational wave function $|j, \bar{\Omega}, m, \epsilon\rangle$ is given by $p = (-1)^{(j-\epsilon/2)}$. Because in a molecular collision the overall parity of the total system must be conserved, a parity change of the rotational wave function is accompanied by a parity change of the radial part of the wave function.[24] The terms "parity-conserving" and "parity-changing" in the present context refer to the parity of the molecular rotational state. For scattering out of the $j = 1/2$ state, an overall parity conservation index can be defined as the ratio of parity-conserving to parity-changing collisions

$$\frac{\sigma_{p\rightarrow p}}{\sigma_{p\rightarrow -p}} \cong \frac{\sigma_{p\rightarrow p}}{\sigma_{-p\rightarrow p}} = (L_{\epsilon_{final}})^p \quad (5)$$

Quasi-Quantum Treatment. The quasi-quantum mechanical treatment (QQT) of inelastic scattering[12,25] employs integrals over angular variables in the kinematic-apse frame to eliminate the sum over coupled equations in orbital angular momentum or impact parameter. The QQT method has been shown to provide a physically compelling explanation for steric asymmetries and parity propensities; these experimental quantities can be straightforwardly and, in the case of hard-shell potentials, quantitatively related to the anisotropy in the interaction.

The spherical angles (γ_a, ϕ_a) of the NO molecular axis with respect to the direction of the kinematic apse $\hat{\mathbf{a}}_k$ provide all of the variables that are relevant to the instantaneous impact at the surface of the hard shell $\mathbf{R_s}(\cos\gamma_a, \phi_a)$ that results in the transfer of an initial state ($j = 1/2$, $\bar{\Omega} = 1/2$, m_a, ϵ) to a final state (j_{final}, $\bar{\Omega}_{final} = 1/2$, $m_{a,final}$, ϵ_{final}).[12,26−28] In the case of a hard-shell potential, the component of the incoming momentum **p** parallel to the surface of the shell will be conserved. Moreover, $\hat{\mathbf{a}}_k$ also coincides with the surface normal at the position of impact, which is assumed to be well-defined due to the elimination of the orbital quantum number l. Therefore $m_a = m_{a,final}$ when one chooses the direction of the m-quantization axis parallel to $\hat{\mathbf{a}}_k$.[29,30]

The scattering amplitude in the apse frame has been shown to emerge from the Feynman path integral

$$g(j,\bar{\Omega},m_a,\epsilon \rightarrow j_{final},\bar{\Omega}_{final},m_{a,final},\epsilon_{final}) = \langle j_{final},\bar{\Omega}_{final},m_{a,final},\epsilon_{final}|g_{j\rightarrow j_{final}}(\gamma_a;\beta)|j,\bar{\Omega},m_a,\epsilon\rangle \quad (6)$$

with

$$g_{j\rightarrow j_{final}}(\gamma_a;\beta) = g(\gamma_a;\beta)e^{i[\eta_{j-jfinal}(\gamma_a;\beta)]} \quad (7)$$

Here $g(\gamma_a;\beta)$, independent of the final and initial rotational state, is taken as the square root of the apse-dependent classical differential scattering cross section $d\sigma/d\omega = d^2\sigma/d(\cos\beta)d\alpha$, where β and α denote the spherical angles of a particular spatial direction of $\hat{\mathbf{a}}_k$ with respect to the incoming momentum **p**

$$g(\gamma_a;\beta) = \frac{2\pi p}{h}\left(\frac{d^2\sigma(\gamma_a)}{d(\cos\beta)d\alpha}\right)^{1/2} \quad (8)$$

where p is the magnitude of the incoming momentum. The QQT hard-shell semi-classical phase shift follows simply from

$$\eta_{j\rightarrow j_{\text{final}}}(\gamma_a;\beta) = \frac{2\pi}{h}\mathbf{R}_s(\cos\gamma_a)\bullet[\mathbf{p}_{\text{final}} - \mathbf{p}] \quad (9)$$

and the allowed magnitude of **p** follows from the rotational energy levels $E(j)$ of the NO molecule. The amount of kinetic energy that is converted into rotation is

$$E(j_{\text{final}}) - E(j) = \frac{p_{\text{final}}{}^2 - p^2}{2\mu} \quad (10)$$

where μ is the reduced mass of the collision system and $p_{\text{final}}{}^2 - p^2$ is the change in the squared magnitude of the momentum.

The differential cross section and the steric asymmetry follow directly from the dimensionless scattering amplitude[12,25]

$$f(j,\bar{\Omega},m_a,\epsilon \rightarrow j_{\text{final}},\bar{\Omega}_{\text{final}},m_{a,\text{final}},\epsilon_{\text{final}}) = \left(\frac{\sin\beta}{\sin\theta}\frac{d\beta}{d\theta}\right)^{1/2} g(j,\bar{\Omega},m_a,\epsilon \rightarrow j_{\text{final}},\bar{\Omega}_{\text{final}},m_{a,\text{final}},\epsilon_{\text{final}}) \quad (11)$$

Here, θ denotes the scattering angle in the center-of-mass system. In order to study orientation effects, as observed experimentally, this scattering amplitude has to be transformed from the apse frame (quantization along a_k) into the laboratory frame (quantization along E).

Previously, the anisotropic hard-shell potentials employed in calculating differential and integral cross sections with QQT have been estimated by using the equipotential contour at the nominal center-of-mass collision energy from ab initio potential energy surfaces.[31,32] In the present work, the shape of the hard-shell potential is fitted to −1 times the experimental values of the steric asymmetry, weighted by their statistical uncertainty plus an estimated ±0.01 systematic contribution to the uncertainty. There is some indication that this systematic contribution may be slightly larger in the case of D_2−NO, based on the predictions of the parity index (see below), where an unweighted fit to SA yields more accurate predictions. The hard shell is parametrized by a five-term Legendre expansion in the angle γ between the N−O bond and the line connecting the molecular centers-of-mass

$$\mathbf{R}_s(\cos\gamma) = \sum_{n=0}^{4} a_n P_n(\cos\gamma) \quad (12)$$

The orientation of the D_2 about its center of mass is neglected. The coefficient of the lowest-order Legendre term, $P_0(\cos\gamma)$, determines overall integral cross sections and does not affect the steric asymmetry; therefore, a_0 is fixed in the fit. The elastic scattering results of Butz et al.[15] suggest that the effective isotropic shell radius is similar for He−NO and D_2−NO. The remaining four coefficients are varied to minimize the square of the difference between the calculated steric asymmetries and −1 times the experimental SA.

Results and Discussion

In Table 1, the experimental steric asymmetries and Λ-doublet propensities of spin-manifold-conserving collisions of NO with D_2 are given, together with their corresponding uncertainty estimates (±2σ precision). The dependence of the measured steric asymmetry on the final rotational and Λ-doublet state is shown in Figure 1. The steric asymmetry is of similar magnitude (or slightly smaller) and of the same sign as that measured for He−NO scattering.[9] The steric asymmetry is largely governed by the repulsive part of the potential,[10] which results in substantial asymmetries for both He−NO and D_2−NO scattering, where repulsion dominates the interaction potential. The steric asymmetry exhibits oscillations with Δj such that $\sigma_{\mathbf{v}\downarrow\uparrow\mathbf{E}} > \sigma_{\mathbf{v}\uparrow\uparrow\mathbf{E}}$ when Δj is even and $\sigma_{\mathbf{v}\downarrow\uparrow\mathbf{E}} < \sigma_{\mathbf{v}\uparrow\uparrow\mathbf{E}}$ when Δj is odd. In general, the behavior of the steric asymmetry is very similar to the behavior for spin-manifold-conserving He−NO collisions. In both cases, the magnitudes of the steric effects are relatively small for low j_{final}, whereas strong oscillations with Δj are observed for higher j_{final}. However, the steric asymmetry is somewhat smaller in scattering with D_2, especially for $\Delta j \leq 7$.

In Figure 1, the steric asymmetries of outgoing e levels ($\epsilon_{\text{final}} = +1$) appear to be shifted upward relative to those of the outgoing f levels ($\epsilon_{\text{final}} = -1$). This means that collisions of NO oriented with the N end toward the incoming D_2 molecule will result in relatively more outgoing molecules residing in an

TABLE 1: Measured Steric Asymmetries SA and Λ-Doublet Propensities L_ϵ for Scattering of NO (j = 1/2; $\Pi_{1/2}$) with D_2[a]

j_{final}	ϵ_{final}	SA (±1σ)	$L_{\epsilon_{\text{final}}}$ (±1σ)
1.5	1	−0.008 ± 0.014	0.39 ± 0.08
1.5	−1	0.007 ± 0.05	4.3 ± 0.5
2.5	1	0.075 ± 0.014	4.4 ± 0.3
2.5	−1	0.019 ± 0.011	0.40 ± 0.07
3.5	1	−0.017 ± 0.010	0.41 ± 0.06
3.5	−1	−0.038 ± 0.012	2.59 ± 0.14
4.5	1	0.242 ± 0.011	3.53 ± 0.17
4.5	−1	0.115 ± 0.008	0.49 ± 0.05
5.5	1	−0.102 ± 0.012	0.37 ± 0.08
5.5	−1	−0.251 ± 0.019	1.82 ± 0.18
6.5	1	0.499 ± 0.009	2.47 ± 0.11
6.5	−1	0.315 ± 0.014	0.58 ± 0.09
7.5	1	−0.373 ± 0.009	0.69 ± 0.07
7.5	−1	−0.407 ± 0.014	1.33 ± 0.11
8.5	1	0.484 ± 0.018	
8.5	−1	0.313 ± 0.012	0.36 ± 0.08
9.5	1	−0.502 ± 0.025	1.30 ± 0.21
9.5	−1	−0.561 ± 0.026	0.96 ± 0.21
10.5	1	0.319 ± 0.042	1.89 ± 0.43
10.5	−1	0.095 ± 0.019	0.22 ± 0.11
11.5	1	−0.525 ± 0.075	0.94 ± 0.54
11.5	−1	−0.585 ± 0.035	1.02 ± 0.26
12.5	1		
12.5	−1	−0.242 ± 0.043	0.81 ± 0.32

[a] The standard deviation of the set of measurements is given (reflecting the (±1σ) precision level).

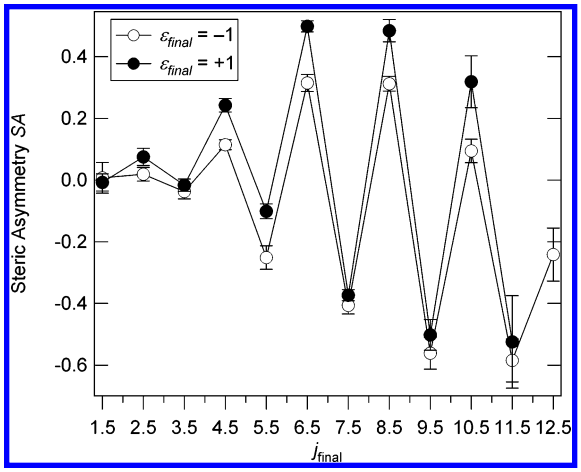

Figure 1. Measured steric asymmetry in spin−orbit-conserving rotationally inelastic collisions of NO (j = 1/2; $\Pi_{1/2}$) with D_2 at 551 cm^{-1} nominal collision energy. The different final Λ-doublet states are shown as open circles ($\epsilon_{\text{final}} = -1$, or f) and filled circles ($\epsilon_{\text{final}} = +1$, or e). Error bars show (±2σ) precision.

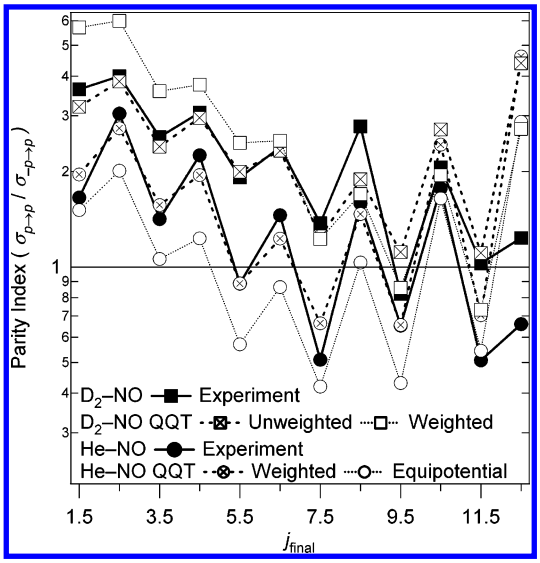

Figure 2. Average measured propensity for parity conservation in inelastic collisions of NO with He[9] and with D_2. The experimental data (solid symbols) are the weighted average of measurements of the parity index for $\epsilon_{final} = +1$ (e) and $\epsilon_{final} = -1$ (f) components of the final j states. Also shown (open symbols and symbols with crosses) are the results of quasi-quantum treatment (QQT) calculations using fitted hard-shell potentials.

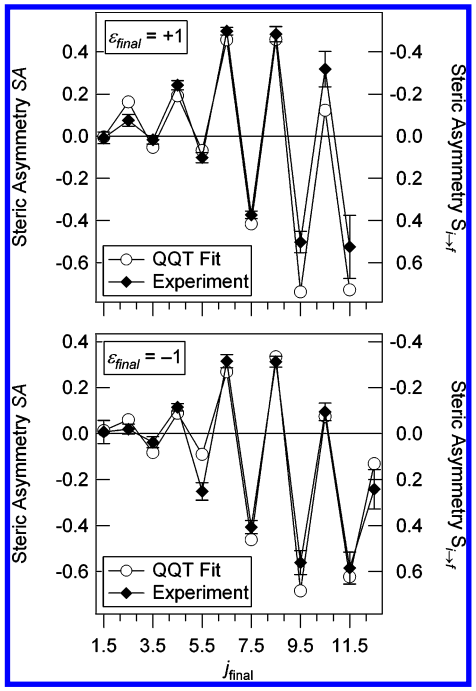

Figure 3. Fit of quasi-quantum calculations of $S_{i\to f}$ (right axis) to −1 times the experimental steric asymmetry SA (left axis), obtained by varying the coefficients in a five-term Legendre expansion for a hard-shell potential. Error bars on SA show ($\pm 2\sigma$) precision; the fits shown are weighted by this precision plus an estimated systematic uncertainty of ±0.01.

e level than when the NO molecule is oriented with the O end toward the incoming molecule. This phenomenon, corresponding to $|SA_{\epsilon_{final}=1}| < |SA_{\epsilon_{final}=-1}|$ when Δj is even and $|SA_{\epsilon_{final}=1}| > |SA_{\epsilon_{final}=-1}|$ when Δj is odd, has also been observed for He−NO scattering[9] and indicates that the collision cross section exhibits a propensity for total parity conservation. Figure 2 shows the parity conservation index (eq 5) for the two collision processes. Values greater than 1 reflect a preference for parity conservation, and values less than 1 reflect a preference for parity breaking. The collisions of NO with He show no propensity for parity conservation for j_{final} values greater than 6.5; the parity index for larger j_{final} states oscillates around 1. Collisions of NO with D_2 clearly display a stronger preference for parity conservation that persists to the highest measured j_{final}.

Because the steric asymmetry is sensitive to the repulsive part of the potential and because the evaluation of cross sections by the QQT method is so rapid, it is easy to fit the shape of a hard-shell potential to optimize the QQT prediction of the steric asymmetry. Figure 3 shows the best fit of the QQT computation of the steric asymmetry obtained by varying the coefficients for the anisotropic components ($n > 0$) in a five-term Legendre expansion for the repulsive potential. For comparison, a similar fit has been carried out for the measured steric asymmetry in the He−NO scattering, for which a high-quality ab initio surface exists.[32] Figure 4 shows a comparison of the shapes for the He−NO hard-sphere potentials that are derived from the steric asymmetry to the equipotential line at the nominal experimental collision energy, which was used to determine the model hard-shell potential in earlier applications of the QQT method.[12,18]

Also shown in Figure 4 is the hard-shell potential derived from the fit to the NO−D_2 steric asymmetries. The Legendre coefficients for hard-shell potentials derived from both He−NO and D_2−NO steric asymmetries are given in Table 2. The even asymmetry of the repulsive interaction, in particular, the P_2 term, is substantially larger in the D_2−NO potential than in the He−NO potential. The even terms in the potential relative

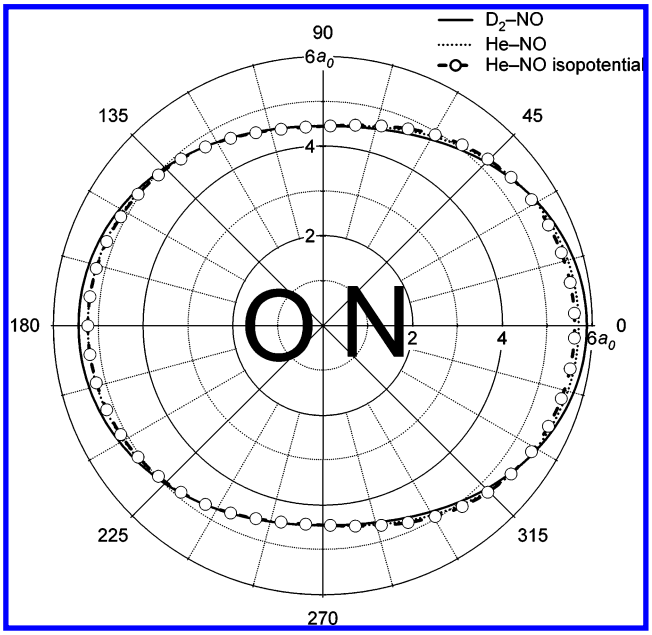

Figure 4. Hard-shell potentials derived from weighted fits to −1 times the measured steric asymmetry and the equipotential line at the nominal experimental He−NO collision energy of 514 cm^{-1}. The N end of the NO molecule is at zero degrees. The radial distance is given in units of the Bohr radius a_0 ($a_0 \cong 52.9$ pm).

to the apse angle γ_a tend to be associated with parity-conserving transitions,[24] and the experimental Λ-doublet propensities in D_2−NO scattering show a larger tendency to preserve parity than in He−NO scattering.[9] The QQT calculations of the parity index, based on the fitted hard-shell potentials, bear out this simple prediction based on the Legendre coefficients. The more the absolute value of the a_2 coefficient exceeds that of the a_1

TABLE 2: Fitted Legendre Coefficients for Hard-Shell Potentials[a]

	a_n	95% confidence interval
He−NO weighted fit to SA		
$n = 1$	0.19	$0.16 < a_1 < 0.22$
$n = 2$	0.72	$0.69 < a_2 < 0.76$
$n = 3$	0.042	$0.015 < a_3 < 0.068$
$n = 4$	−0.11	$-0.18 < a_4 < -0.04$
D_2−NO weighted fit to SA		
$n = 1$	0.143	$0.10 < a_1 < 0.18$
$n = 2$	0.813	$0.76 < a_2 < 0.86$
$n = 3$	0.0775	$0.058 < a_3 < 0.097$
$n = 4$	−0.0062	$-0.11 < a_4 < 0.096$
D_2−NO unweighted fit to SA		
$n = 1$	0.155	$0.11 < a_1 < 0.20$
$n = 2$	0.809	$0.77 < a_2 < 0.85$
$n = 3$	0.0790	$0.055 < a_3 < 0.107$
$n = 4$	−0.0775	$-0.15 < a_4 < 0.0006$

[a] The 95% confidence range is given in the final column. The coefficient of the P_0 term for both systems is fixed at $a_0 = 4.864$, taken from a Legendre expansion of the ab initio He−NO isopotential at the nominal collision energy. For comparison, the Legendre moments from the ab initio He−NO isopotential are $a_1 = 0.198$, $a_2 = 0.691$, $a_3 = -0.013$, $a_4 = -0.150$, $a_5 = -0.0012$, $a_6 = 0.0263$.

coefficient, the more the parity index will tend to remain greater than 1 for large values of j_{final}. Note that the a_1 and a_2 coefficients dominate the anisotropy for both He−NO and D_2−NO. The calculations, shown as the crossed open symbols in Figure 2, show a substantial preference for parity conservation in the D_2−NO scattering for all j_{final}, whereas the QQT calculations on the fitted He−NO potential, with its slightly less prominent even anisotropy, loses parity preference above $j_{final} = 5.5$. A measure of the sensitivity of the parity index to the shape of the potential is given by the comparison of the He−NO parity index calculated using the hard shell from the weighted fit to the index calculated using a hard shell at the equipotential line at the nominal collision energy (also shown in Figure 2). Even the small difference in the shapes of the potential yields a substantial difference in the predicted parity index. Furthermore, the hard shell resulting from an unweighted fit to the measured SA for D_2−NO, which is well within the uncertainties of the weighted fit, gives markedly improved predictions of the parity index.

The alternation in parity preference with Δj, which becomes more prominent at high j_{final}, is easily rationalized by considering the dominant Legendre terms in the QQT expression for the scattering amplitude. The differential cross section for scattering of state-selected NO ($|j\ m_j\ \bar{\Omega}\ \epsilon\rangle = |1/2\ \pm 1/2\ 1/2\ -1\rangle$) into a final state of given j_{final} and parity ϵ_{final} is dominated by a single Legendre term in the apse angle γ_a[12]

$$\frac{d\sigma}{d\omega} \propto \left| \int_{-1}^{1} d(\cos\gamma_a)\, P_{j_{final}+(\epsilon_{final}/2)}(\cos\gamma_a)\, g_{j\to j_{final}}(\gamma_a;\beta) \right|^2 \quad (13)$$

where the factor $g_{j\to j_{final}}(\gamma_a;\beta)$ includes the classical scattering amplitude and the semiclassical phase shift (see eq 7). Therefore, the contribution to a given value of j_{final} will include a single Legendre moment of the phase shift function $g_{j\to j_{final}}(\gamma_a;\beta)$ of order $\Delta j = (j_{final} - 1/2)$ for $\epsilon_{final} = -1$ and one moment of order $\Delta j + 1 = (j_{final} + 1/2)$ for $\epsilon_{final} = +1$. Qualitative conclusions can be drawn for large j_{final} by assuming that the magnitude of the angle-averaged Legendre term tends to be smaller for larger values of n because of averaging over more oscillations near the stationary phase region,[12] meaning that for a given Δj, the $P_{\Delta j}(\cos\gamma_a)$ term (i.e., $\epsilon_{final} = -1$) will be larger than the $P_{\Delta j+1}(\cos\gamma_a)$. This term corresponds to parity conservation for even Δj and to parity breaking for odd Δj. This is the parity propensity exhibited by He−NO and D_2−NO scattering in Figure 2; for even Δj, the larger $P_{\Delta j}(\cos\gamma_a)$ term appears in the numerator, making the parity index >1; for odd

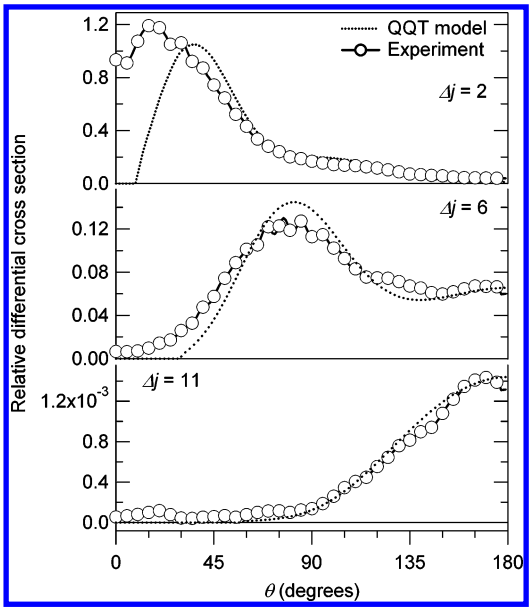

Figure 5. Comparison of experiment[18] and QQT calculations on fitted hard-shell potentials for selected parity-conserving differential cross sections in the scattering of state-selected NO ($|j\ m_j\ \bar{\Omega}\ \epsilon\rangle = |1/2\ \pm 1/2\ 1/2\ -1\rangle$) with He. The agreement of the calculated differential cross sections using the fitted potential is similar to that observed in QQT calculations[25] using the equipotential line at 514 cm^{-1} from the ab initio potential of Kłos et al.[32] The cross sections are normalized to the close-coupled calculated cross section.

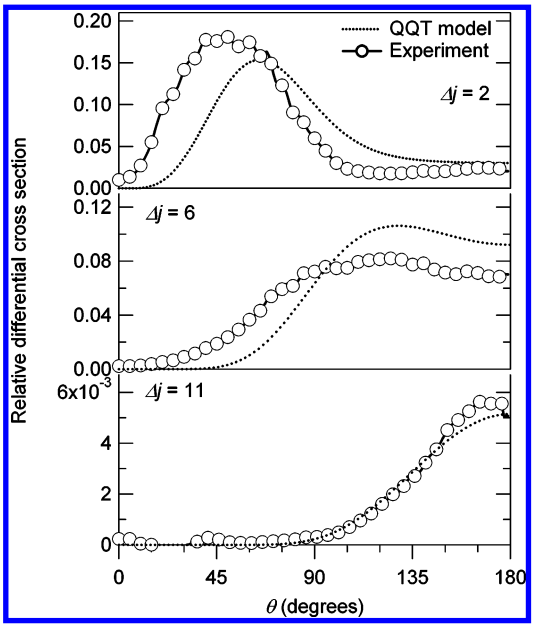

Figure 6. Comparison of experiment[18] and QQT calculations on fitted hard-shell potentials for selected parity-breaking differential cross sections in the scattering of state-selected NO ($|j\ m_j\ \bar{\Omega}\ \epsilon\rangle = |1/2\ \pm 1/2\ 1/2\ -1\rangle$) with He. The agreement of the calculated differential cross sections using the fitted potential is similar to that observed in QQT calculations[25] using the equipotential line at 514 cm^{-1} from the ab initio potential of Kłos et al.[32] The cross sections are normalized to the close-coupled calculated cross section.

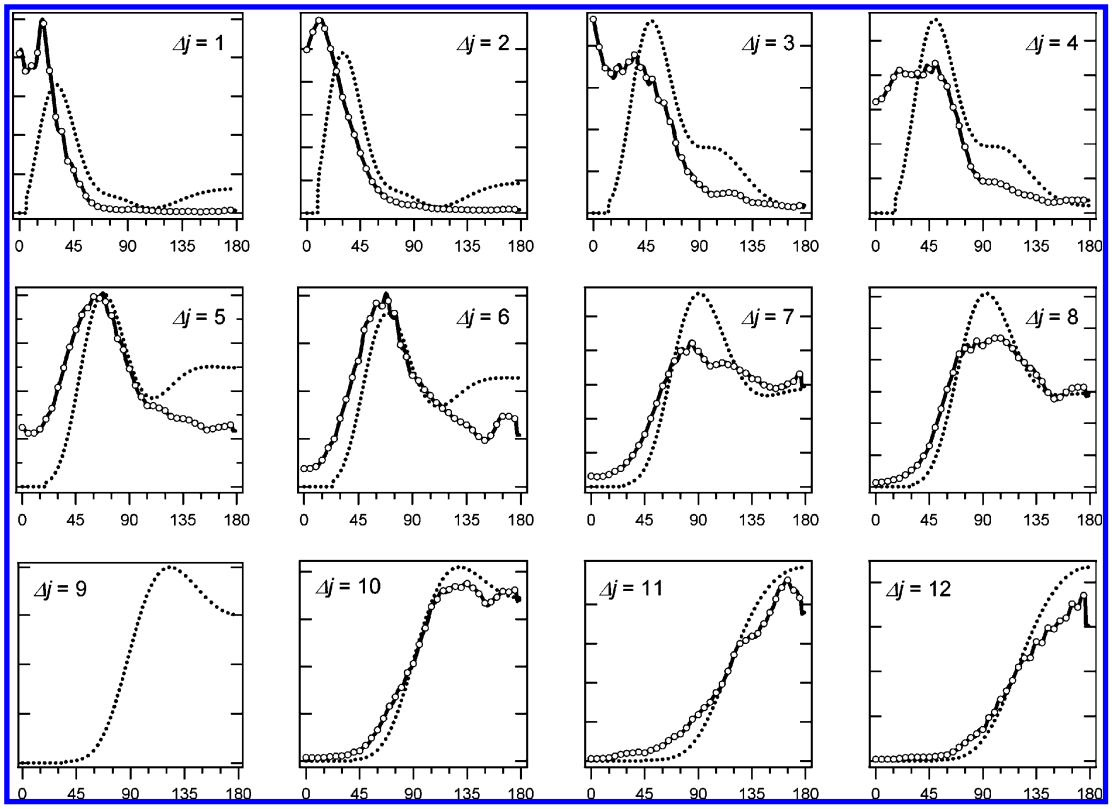

Figure 7. Comparison of experimental[18] and calculated relative differential cross sections for parity-conserving NO ($|j\ m_j\ \bar{\Omega}\ \epsilon\rangle = |1/2\ \pm 1/2\ 1/2\ -1\rangle$) scattering from D_2. Calculated cross sections from QQT using the hard-shell potential derived from the unweighted fit to the measured steric asymmetry are given as the dotted line; experimental cross sections are given as the heavy solid lines and open circles (circles are placed on every fifth experimental data point).

Δj, the $P_{\Delta j}(\cos\gamma_a)$ term appears in the denominator, making the parity index <1. The D_2-NO scattering shows an additional overall preference for parity conservation that does not appear for He−NO above $j_{final} = 5.5$.

The QQT calculations using the fitted hard-shell potentials provide good predictions of the parity index in NO−He and D_2-NO scattering. The question remains how well the fitted anisotropy will reproduce other physical phenomena that are sensitive to the shape of the repulsive wall. In particular, the shape of the differential cross section is a stringent test of the shape of the potential energy surface. Differential cross sections have been measured for scattering of fully state-selected NO ($|j\ m_j\ \bar{\Omega}\ \epsilon\rangle = |1/2\ \pm 1/2\ 1/2\ -1\rangle$) with He[17] and with D_2,[18] and both full close-coupling and QQT calculations of differential cross sections for fully state-selected He−NO scattering have been carried out,[9,25] based on the ab initio potential of Kłos and co-workers.[32] Close-coupling calculations on an accurate surface provide excellent agreement with the measured differential cross sections, as has also been seen for quantum-state resolved scattering of Ar−NO using non-state-selected beams.[33,34]

The QQT calculations deviate systematically from the close-coupled calculations in a way that reflects the assumptions of the QQT method.[25] For example, QQT uses classical angle-dependent scattering amplitudes in conjunction with the semi-classical phase shift; this treatment implicitly assumes that the hard shell is much larger than the relevant de Broglie wavelength and hence does not include diffraction effects. Diffraction is especially important for forward scattering, and the QQT calculations fail to reproduce the forward-scattered peaks at low j_{final}.[25] Representative QQT calculations for He−NO, using the fitted hard-shell potential, are compared to experimental differential cross sections in Figures 5 and 6. The calculations on the fitted potential are similar to those using a hard shell at the 514 cm^{-1} equipotential line of the ab initio surface,[25] showing less forward scattering than the experiment and showing improved agreement at higher j_{final}, where backward scattering dominates. The fitted hard-shell potential shows a significant difference from the 514 cm^{-1} equipotential line of the ab initio surface only in the $P_3(\cos\gamma)$ term as defined by eq 12 (see Table 2). Note that the equipotential line consists of a larger Legendre expansion using 7 terms.

The anisotropy in the He−NO and the D_2-NO systems was empirically estimated by Westley et al.,[16] who used a two-dimensional hard-ellipse model to predict the classical differential cross section, applying the formulas of Bosanac and Buck.[35] Optimizing the parameters of the model potential to produce the best agreement with their experimental He−NO measurements yielded a markedly larger anisotropy than the ab initio surface calculated by Yang and Alexander[36] under the coupled-electron-pair approximation (CEPA). The Yang and Alexander surface also predicts scattering angles farther in the backward direction than the experimental observation. The coupled-cluster (RCCSD(T)) potential of Kłos et al.[32] shows a stronger anisotropy in the repulsive wall, and close-coupling calculations of scattering on this surface accurately predict the differential cross sections for He−NO scattering.[17] Fitting the potential to the steric asymmetry appears to accurately yield the anisotropy of the repulsive wall for NO−He scattering, as judged by comparison to the RCCSD(T) ab initio surface.[25,32]

Figures 7 and 8 show similar comparisons of the experimental and QQT-calculated differential cross sections for D_2-NO scattering. The differential cross sections are relatively well-

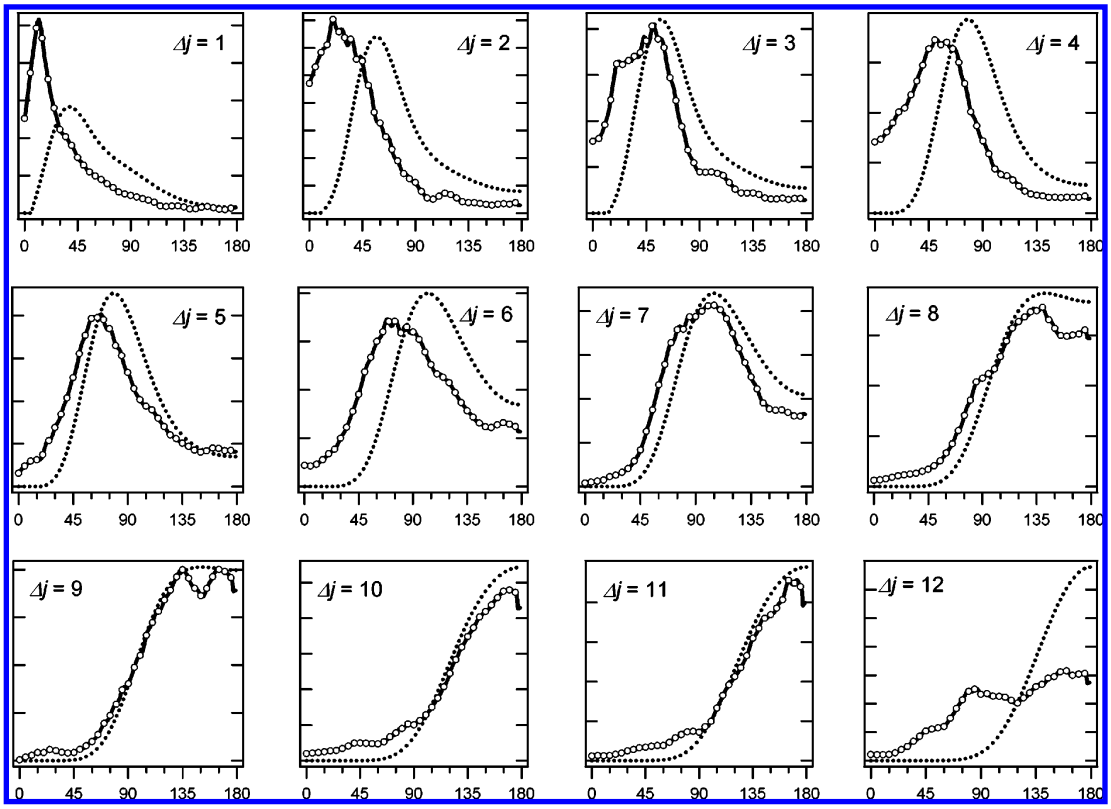

Figure 8. Comparison of experimental[18] and calculated differential cross sections for parity-breaking NO ($|j\ m_j\ \bar{\Omega}\ \epsilon\rangle = |1/2\ \pm 1/2\ 1/2\ -1\rangle$) scattering from D_2. Calculated cross sections from QQT using the hard-shell potential derived from the unweighted fit to the measured steric asymmetry are given as the dotted line; experimental cross sections are given as the heavy solid lines and open circles (circles are placed on every fifth experimental data point).

reproduced by the QQT calculations on the fitted hard-shell surface (the unweighted fit is shown; the predictions with the weighted fit are slightly poorer), with deviations similar to those in the He−NO case, again principally from the assumptions of the QQT method. In interpreting their elastic scattering results, Butz et al.[15] found that D_2−NO required a composite Lennard-Jones (6,3)−(24,6) potential, whereas the He−NO was satisfactorily modeled using a (12,6) potential, suggesting differences between D_2−NO and He−NO in the inner (hard-shell boundary) part of the potential. Westley et al.,[16] in their hard-ellipse fits to the differential cross section data, found a larger anisotropy for the D_2−NO than that for the He−NO. A similar conclusion was drawn by Gijsbertsen et al.[17] from analogous fits to their data. The fit to the steric asymmetry measurement confirms this interpretation and, judging from the predicted differential cross sections, seems to accurately capture the shape of the repulsive wall of the D_2−NO potential, at least within the approximations inherent in the QQT method. This fitted repulsive shell for the D_2−NO system has a larger even anisotropy than the corresponding He−NO system.

Conclusions

The steric asymmetry and parity propensity for rotationally inelastic, spin−orbit-conserving collisions of state-selected NO with D_2 have been measured in crossed-molecular-beam studies at a nominal collision energy of 551 cm^{-1}. An effective hard-shell interaction has been derived from fits of quasi-quantum calculations to the measured steric asymmetry. An analogous fitting procedure reproduces the ab initio repulsive wall for He−NO, and the fitted D_2−NO hard shell yields reasonably accurate predictions of differential cross sections for inelastic scattering.

Acknowledgment. The authors thank Rob Kortekaas for the outstanding technical support that made these experiments possible and Dr. Albert Ballast for his interest and helpful discussions. The Netherlands Organization for Scientific Research (NWO) is gratefully acknowledged for financial support of this work through CW and FOM. Craig A. Taatjes is supported by the Division of Chemical Sciences, Geosciences, and Biosciences, the Office of Basic Energy Sciences, the U.S. Department of Energy, and his participation was partially facilitated by a NATO collaborative travel grant. Sandia is a multiprogram laboratory operated by Sandia Corporation, a Lockheed Martin Company, for the United States Department of Energy's National Nuclear Security Administration under Contract DE-AC04-94-AL85000.

References and Notes

(1) Nizamov, B.; Dagdigian, P. J.; Alexander, M. H. *J. Chem. Phys.* **2001**, *115*, 8393.
(2) van den Ende, D.; Stolte, S. *Chem. Phys. Lett.* **1980**, *76*, 13.
(3) Kuipers, E. W.; Tenner, M. G.; Kleyn, A. W.; Stolte, S. *Nature* **1988**, *334*, 420.
(4) de Lange, M. J. L.; van Leuken, J. J.; Drabbels, M. M. J. E.; Bulthuis, J.; Snijders, J. G.; Stolte, S. *Chem. Phys. Lett.* **1998**, *294*, 332.
(5) van Leuken, J. J.; Bulthuis, J.; Stolte, S.; Snijders, J. G. *Chem. Phys. Lett.* **1996**, *260*, 595.
(6) de Lange, M. J. L.; Drabbels, M.; Griffiths, P. T.; Bulthuis, J.; Stolte, S.; Snijders, J. G. *Chem. Phys. Lett.* **1999**, *313*, 491.
(7) Tenner, M. G.; Kuipers, E. W.; Kleyn, A. W.; Stolte, S. *J. Chem. Phys.* **1991**, *94*, 5197.
(8) Schreel, K.; ter Meulen, J. J. *J. Phys. Chem. A* **1997**, *101*, 7639.
(9) de Lange, M. J. L.; Stolte, S.; Taatjes, C. A.; Kłos, J.; Groenenboom, G. C.; van der Avoird, A. *J. Chem. Phys.* **2004**, *121*, 11691.

(10) Alexander, M. H.; Stolte, S. *J. Chem. Phys.* **2000**, *112*, 8017.
(11) Gijsbertsen, A.; de Lange, M. J. L.; Wiskerke, A. E.; Linnartz, H.; Drabbels, M.; Kłos, J.; Stolte, S. *Chem. Phys.* **2004**, *301*, 293.
(12) Gijsbertsen, A.; Linnartz, H.; Taatjes, C. A.; Stolte, S. *J. Am. Chem. Soc.* **2006**, *128*, 8777.
(13) Gijsbertsen, A.; Linnartz, H.; Kłos, J.; Stolte, S. *Phys. Scr.* **2005**, *72*, C1.
(14) Langhoff, S. R.; Bauschlicher, C. W.; Partridge, H. *Chem. Phys. Lett.* **1994**, *223*, 416.
(15) Butz, H. P.; Feltgen, R.; Pauly, H.; Vehmeyer, H. *Z. Phys.* **1971**, *247*, 70.
(16) Westley, M. S.; Lorenz, K. T.; Chandler, D. W.; Houston, P. L. *J. Chem. Phys.* **2001**, *114*, 2669.
(17) Gijsbertsen, A.; Linnartz, H.; Rus, G.; Wiskerke, A. E.; Stolte, S.; Chandler, D. W.; Kłos, J. *J. Chem. Phys.* **2005**, *123*, 224305.
(18) Gijsbertsen, A.; Linnartz, H.; Stolte, S. *J. Chem. Phys.* **2006**, *125*, 133112.
(19) van Leuken, J. J.; van Amerom, F. H. W.; Bulthuis, J.; Snijders, J. G.; Stolte, S. *J. Phys. Chem.* **1995**, *99*, 15573.
(20) de Lange, M. J. L. Steric and State-to-State Dependence of Rotationally Inelastic Scattering of NO. Ph.D. Dissertation, Vrije Universiteit, Amsterdam, The Netherlands, 2003.
(21) Cline, J. I.; Lorenz, K. T.; Wade, E. A.; Barr, J. W.; Chandler, D. W. *J. Chem. Phys.* **2001**, *115*, 6277.
(22) Meyer, H. *J. Chem. Phys.* **1995**, *102*, 3151.
(23) Kim, H.; Meyer, H. *Chem. Phys.* **2004**, *301*, 273.
(24) Alexander, M. H. *Faraday Discuss.* **1999**, *113*, 437.
(25) Ballast, A.; Gijsbertsen, A.; Linnartz, H.; Taatjes, C. A.; Stolte, S. A Quasi-Quantum Treatment of Inelastic Molecular Collisions; 25th International Symposium on Rarefied Gas Dynamics, St. Petersburg, Russia, 2006.
(26) Evans, G. T.; She, R. S. C.; Bernstein, R. B. *J. Chem. Phys.* **1985**, *82*, 2258.
(27) She, R. S. C.; Evans, G. T.; Bernstein, R. B. *J. Chem. Phys.* **1986**, *84*, 2204.
(28) Hoffman, D. K. *J. Chem. Phys.* **1969**, *50*, 4823.
(29) Hoffman, D. K.; Evans, J. W.; Kouri, D. J. *J. Chem. Phys.* **1984**, *80*, 144.
(30) McGuire, P.; Kouri, D. J. *J. Chem. Phys.* **1974**, *60*, 2488.
(31) Alexander, M. H. *J. Chem. Phys.* **1999**, *111*, 7426.
(32) Kłos, J.; Chalasinski, G.; Berry, M. T.; Bukowski, R.; Cybulski, S. M. *J. Chem. Phys.* **2000**, *112*, 2195.
(33) Elioff, M. S.; Chandler, D. W. *J. Chem. Phys.* **2002**, *117*, 6455.
(34) Kohguchi, H.; Suzuki, T.; Alexander, M. H. *Science* **2001**, *294*, 832.
(35) Bosanac, S.; Buck, U. *Chem. Phys. Lett.* **1981**, *81*, 315.
(36) Yang, M.; Alexander, M. H. *J. Chem. Phys.* **1995**, *103*, 6973.